ROTATING-FRAME RELAXATION STUDIES OF SLOW MOTIONS IN FLUORINATED PHOSPHOLIPID MODEL MEMBRANES

ZHENG-YU PENG,*‡ VIRGIL SIMPLACEANU,‡ IRVING J. LOWE,‡§ AND CHIEN HO‡
*Department of Physics and ‡Department of Biological Sciences, Carnegie Mellon University, Pittsburgh, Pennsylvania 15213; and §Department of Physics and Astronomy, University of Pittsburgh, Pittsburgh, Pennsylvania 15260

ABSTRACT Rotating-frame relaxation experiments have been carried out on ^{19}F-labeled dimyristoylphosphatidylcholine model membranes. The lipids are labeled with a single CF_2 group in the 4-, 8-, or 12-position of the 2-acyl chain. Both oriented lipid bilayers and multilamellar liposomes have been investigated. The relaxation rate has been measured as a function of the locking-field strength, the sample orientation, the label position, and the temperature. Our results have confirmed that extensive slow motions exist in the bilayer and dominate the low-frequency relaxation. The relaxation rate is quite sensitive to the label position. However, many other features of the relaxation are very similar for all three lipid isomers. The temperature dependence of the relaxation rate for the multilamellar liposomes differs from the oriented bilayers, which may imply that the motions are also different. To fit our data, a working model consisting of a superposition of an anisotropic reorientation term and a director fluctuation term has been proposed. We have also verified that almost all of the relaxation process is caused by modulations of the intramolecular interactions. Based on this, a view of the slow motions at a molecular level is discussed in this paper.

INTRODUCTION

Phospholipid bilayers are the main structural matrix of biological membranes. A knowledge of the molecular packing and dynamics of phospholipids is essential for an understanding of various membrane functions. During the last decade, a large number of nuclear magnetic resonance (NMR) studies on phospholipid model membranes have been carried out by various investigators (for example, see Seelig and Seelig, 1980; Griffin, 1981; Davis, 1983; Ho et al., 1985 and the references therein). At present, the static properties of the lipid bilayer, such as the packing and ordering of the lipid molecules, are reasonably well characterized. Dynamic processes involving lipid molecules are, however, less understood. This is especially true when considering the slow molecular motions of the lipids, which could play an important role in lipid-protein interactions (for example, see Feigenson and Chan, 1974; Cornell et al., 1982; Smith and Oldfield, 1984).

The slow molecular motions of phospholipids have been investigated by NMR using line-shape analysis (Campbell et al., 1979; Huang et al., 1980), spin-lattice relaxation either in low to medium magnetic fields or in the rotating frame (Fisher and James, 1978; Cornell and Pope, 1980; Pope et al., 1982; Kimmich et al., 1983; Brown et al., 1983 and 1986), and spin–spin relaxation (Bloom and Sternin, 1987). Previous relaxation studies of slow motions have led to a few controversial conclusions. First, the dispersions of spin–lattice relaxation rate (T_1^{-1}) of proton for multilamellar liposomes at low field (Kimmich et al., 1983), and of ^2H and ^{13}C nuclei for unilamellar vesicles at higher field (Brown et al., 1983 and 1986) have showed only a relatively weak dependence on the magnetic field (H_0), which indicates that the motions are "collective," or, equivalently, a broad distribution of motional correlation times would be needed to explain the data. This is also true in the case of the rotating-frame relaxation rate ($T_{1\rho}^{-1}$) versus the locking field (H_1) for multilamellar liposomes (Fisher and James, 1978). Secondly, the locking-field dependence of the proton rotating-frame spin-lattice relaxation rate of oriented lipid bilayers (Cornell and Pope, 1980; Pope et al., 1982) has been found to be well fitted by the conventional Lorentzian relaxation model with a single correlation time, and, combined with the orientation dependence of the relaxation rate, these data have been interpreted in terms of relaxation through a modulation of intermolecular interactions (Pope et al., 1982).

In this paper, we report a ^{19}F rotating-frame spin-lattice relaxation investigation of both oriented bilayers and multilamellar liposomes prepared from fluorinated dimyristoylphosphatidylcholines (DMPC). The results obtained from these two types of samples under the same experi-

Address all correspondence to Dr. Chien Ho, Department of Biological Sciences, Carnegie Mellon University, 4400 Fifth Avenue, Pittsburgh, PA 15213.

mental conditions are then compared. The use of oriented bilayers allows us to study the orientation dependence of the relaxation rate in addition to the field and temperature dependence. Theoretically, these reflect different aspects of the dynamical properties of the system. The orientation dependence is more sensitive to the character of molecular motion, whereas the field dependence is more sensitive to the distribution of correlation times. Both types of information are clearly crucial to our understanding of lipid dynamics in model membranes.

The fluorine-containing lipids used in this work (DMPCs fluorinated at 4-, 8-, or 12-position of the 2-acyl chain) have been synthesized and previously studied in our laboratory (Engelsberg et al., 1982; Post et al., 1984; Dowd et al., 1984). They can be used as bilayer probes which have both high NMR sensitivity and label specificity. The ^{19}F labeling has several advantages that can simplify the investigation of molecular motions in lipid bilayers. Clearly, one has the ability to monitor the slow motions at a specific chain position, thus the model fitting can be more precise and changes of the motion along the acyl chain can be observed. Previous relaxation experiments covering a similar time scale were limited to the ^1H nucleus, which can only give relaxation rates averaged over the entire molecule, because many of the individual proton resonances overlap (Fisher and James, 1978; Cornell and Pope, 1980; Pope et al., 1982; Kimmich et al., 1983). Another advantage is that the large chemical shift anisotropy (CSA) of the CF_2 group allows us to consider only the intramolecular interactions in analyzing our relaxation data.

Although relaxation measurements are most sensitive to the motional spectral density function at a specific frequency, in recognition of the complexity of the system, it is very likely that a number of different motions coexist and are responsible for the total relaxation behavior. Some of the motions can be spatially localized, some can be collective, whereas some motions may affect only a small number of molecules, such as motions occurring around packing defects. Experimentally, it is found that the presence of more than one type of motion is required to explain our results on both the orientation and the locking-field dependence. The present characterization of the slow motions in pure lipid model membranes will serve as a starting point for subsequent studies of complex protein-lipid mixtures, aiming towards a more realistic model of biological membranes.

MATERIALS AND METHODS

Materials

1-Myristoyl-2-[8,8-difluoromyristoyl]-*sn*-glycero-3-phosphatidylcholine (2-[8,8-$^{19}F_2$]DMPC), and the corresponding 2-[4,4-$^{19}F_2$] and 2-[12,12-$^{19}F_2$] difluoro derivatives were synthesized as described previously (Engelsberg et al., 1982). The main phase transition temperatures of the 2-[4,4-$^{19}F_2$]DMPC, 2-[8,8-$^{19}F_2$]DMPC, and 2-[12,12-$^{19}F_2$]DMPC are 24, 18, and 14°C, respectively (J. M. Sturtevant, S. R. Dowd, and C. Ho, unpublished results). The purity of the lipids was checked before use by thin-layer chromatography (TLC). The perdeuterated DMPC-d_{54} was obtained from Avanti Polar Lipids, Inc., Birmingham, AL. All other chemicals used were reagent grade from commercial suppliers and used without further purification.

Preparation of Oriented Bilayers

About 30 mg of ^{19}F-labeled lipid was dissolved in 0.6 ml 3:1 chloroform/methanol solvent; 20-μl aliquots were deposited on each microscope coverslip (thickness No. 2, cut to 7.8 mm × 22 mm, Fisher Scientific Co., Pittsburgh, PA), and dried under vacuum for at least 12 h. About 30 slips were then stacked as a sandwich and incubated in a closed chamber at 32°C and 90 ± 2% relative humidity (in the presence of 1 M $MgCl_2$ aqueous solution as the humidity control) for 3–7 d during which the lipid molecules hydrate and gradually orient. A finished sample is optically transparent, and is sealed in a square sample cell.

Defects Characterization

Several kinds of packing defects have been observed in the oriented bilayers (Asher and Pershan, 1979; Tanaka and Freed, 1984). Because the unoriented part of the sample will give a powder pattern instead of a Pake doublet in the ^{19}F NMR spectrum and will have no orientation dependence, one can judge the sample quality by taking a control spectrum. The unoriented lipid in our sample was always <5%. A preliminary characterization of our oriented samples was made by using a polarizing microscope. A typical sample consists of large oriented areas separated by line defects which we call domain walls. Within the oriented areas, very fine, homogeneously distributed, dotlike defects can be observed under certain conditions. Similar dotlike defects have been documented before (Tanaka and Freed, 1984). They seem to be sensitive to mechanical dilation as well as to changes in temperature and water content.

Preparation of Multilamellar Liposomes

^{19}F-labeled lipid was dispersed in deionized water at a 30:70 wt/wt ratio and vortexed thoroughly at 32°C for 15–60 min. Sometimes two to three freeze-and-thaw cycles were included to eliminate small vesicles. The homogeneity of the sample was judged by visual inspection (milklike) and by the absence of any sharp resonance in the ^{19}F NMR spectrum.

NMR Measurements

Rotating-frame relaxation rate measurements were carried out with homemade probes, using the standard spin-locking method, on a modified WH-300 spectrometer (Bruker Instruments, Inc., Billerica, MA) operating at 282.4 MHz for ^{19}F. The length of the 90° pulse was 2.2 μs for the probe used in the liposome work and 3.2 μs for the probe used for oriented bilayers. The locking-field (H_1) intensities were controlled by an electronic attenuator and calibrated by measuring the corresponding 360° pulse durations. For the relaxation measurements, the locking field was varied from 1 to 10 Gauss. The carrier frequency of the transmitter was adjusted to the center of the dipolar line for the oriented bilayers. The line shape for multilamellar liposomes is more complicated due to a large CSA for CF_2, so the carrier frequency was placed in the center of gravity of the powder pattern.

All NMR experiments were carried out under conditions such that the lipids were in the liquid crystalline (L_α) phase, which could be verified by taking control spectra. All measurements were done at 32 ± 1°C unless otherwise stated. A typical measurement consisted of 12 locking times, with 64–256 transients accumulated for each time. To avoid heating the sample, the duty factor of the spin-locking sequence was limited to successively smaller values when increasing the locking-field strength. At least two independent measurements were made for each locking field or orientation. The degradation of the lipids during the sample preparation

and the measurement periods was <5%, and the relaxation time was reproducible within the experimental error.

Recorded free-induction decays (FID) were multiplied by a matched numerical Gaussian filter to maximize the signal-to-noise ratio and then integrated; the results were fitted with a single exponential function by a nonlinear least-squares fit to extract the relaxation times. The error for the relaxation times was less than ±10% estimated from repeated measurements. In the low locking-field and 0° orientation, because the relaxation times are extremely short, the error could be somewhat larger.

THEORETICAL BACKGROUND

The rotating-frame relaxation rate can be calculated theoretically provided that one knows both the motion and the relaxation pathway.

1. Relaxation via Fluctuating Chemical Shift Anisotropy

Because the CF_2 group has a large CSA (Dowd et al., 1984), the CSA is expected to be the dominant relaxation mechanism for the motions that modulate the intramolecular interactions. The intermolecular dipolar interactions can only become important if the motions are pure translations, which keep the CSA tensor as a constant during the motion. This possibility can be excluded further by the results of dilution experiments (*vide infra*). For simplicity, in the following we shall assume that the relaxation is caused by the fluctuations of the CSA only. The intramolecular dipolar interactions (homonuclear F-F and heteronuclear F-H) are much smaller than the CSA (Wu et al., 1985), so that their contribution to the motion-induced relaxation will not be significant compared with CSA.

The NMR relaxation rates in the laboratory frame and in the rotating frame, due to the anisotropic chemical shift, have been calculated by Blicharski (1972). We will follow the formalism developed by Blicharski with emphasis on the orientation and the locking-field dependence of the relaxation rate for an anisotropic medium.

The CSA Hamiltonian can be written as (in frequency units)

$$\mathcal{H} = \gamma \sum_{pq} I_p \sigma_{pq} H_q, \tag{1}$$

where σ_{pq} is the CSA tensor in the Cartesian coordinate ($p, q = x, y, z$), I_p is the nuclear spin operator along the p axis, and H_q is the magnetic field along the q axis. Because of the existence of fast motions that are axially symmetric about the molecular long axis, the CSA tensor is reduced to an axially symmetric effective CSA tensor with no off-diagonal elements. In the molecule frame, we have

$$\underline{\underline{\sigma}} = \begin{bmatrix} -\frac{1}{2}\sigma_{eff} & 0 & 0 \\ 0 & -\frac{1}{2}\sigma_{eff} & 0 \\ 0 & 0 & \sigma_{eff} \end{bmatrix} \tag{2}$$

and σ_{eff} can be represented by (Ho et al., 1985):

$$\sigma_{eff} = \frac{2}{3} \sum_{kl} S_{kl}^{FM} \sigma_{kl}^{rig}, \tag{3}$$

where σ_{kl}^{rig} are elements of the rigid lattice chemical shift tensor, and S_{kl}^{FM} are fast motion order parameters which characterize the averaging effect of fast motions. By rewriting $\underline{\underline{\sigma}}$ in the spherical tensor form

$$\begin{cases} F_{20}^{mol} = \sigma_{zz} = \sigma_{eff} \\ F_{2\pm1}^{mol} = \mp \frac{1}{\sqrt{6}} [(\sigma_{xz} + \sigma_{zx}) \pm i(\sigma_{yz} + \sigma_{zy})] = 0 \\ F_{2\pm2}^{mol} = \frac{1}{\sqrt{6}} [(\sigma_{xx} - \sigma_{yy}) \pm i(\sigma_{xy} + \sigma_{yx})] = 0 \end{cases} \tag{4}$$

and transforming it into the laboratory frame, we obtain

$$F_{2m}^{lab} = \sum_{m'} F_{2m'}^{mol} D_{m'm}^{(2)}(\Omega) = \sigma_{eff} D_{0m}^{(2)}(\Omega), \tag{5}$$

where $D_{m'm}^{(2)}(\Omega)$ are the Wigner rotation matrices, and Ω represents the Euler angles which define the transform from the molecule frame to the laboratory frame. As Blicharski (1972) did, we define the static magnetic field as $\boldsymbol{H} = \boldsymbol{n}H_0$, where $\boldsymbol{n} = (0, 0, 1)$ is a unit vector along the z axis in the laboratory frame. We can then construct the second-order spin tensor operator A_{2m} as follows.

$$\begin{cases} A_{20}^{lab} = \frac{2}{\sqrt{6}} I_z n_z + \frac{1}{\sqrt{6}} (I_1 n_{-1} + I_{-1} n_1) = \frac{2}{\sqrt{6}} I_z \\ A_{2\pm1}^{lab} = \frac{1}{\sqrt{2}} (I_{\pm1} n_z + I_z n_{\pm1}) = \frac{1}{\sqrt{2}} I_{\pm1} \\ A_{2\pm2}^{lab} = I_{\pm1} n_{\pm1} = 0, \end{cases} \tag{6}$$

where

$$I_{\pm1} = \frac{\mp1}{\sqrt{2}} (I_x \pm I_y) \quad \text{and} \quad n_{\pm1} = \frac{\mp1}{\sqrt{2}} (n_x \pm n_y). \tag{7}$$

The CSA Hamiltonian becomes

$$\mathcal{H} = \left(\gamma H_0 \sqrt{\frac{3}{2}}\right) \sum_m (-1)^m A_{2m}^{lab} F_{2-m}^{lab}$$

$$= \omega_{CSA} \sum_m (-1)^m D_{0-m}^{(2)}(\Omega) A_{2m}^{lab}, \tag{8}$$

where

$$\omega_{CSA} = \frac{\sqrt{6}}{2} \gamma \sigma_{eff} H_0. \tag{9}$$

We will derive the rotating-frame relaxation rate using the above Hamiltonian and the standard perturbation method (Abragam, 1961). The weak collision theory is valid if the motional correlation time is short or if the locking field H_1 is greater than the fluctuating part of the

interaction. Because we are dealing with slow motions, short correlation time cannot be assumed. From the strength of the total CSA interaction (and to a lesser amount, the total dipolar interaction), we find that the second condition also does not hold if we compare the total Hamiltonian with the low-locking field that we have used. However, the fluctuating part of the interaction can be much smaller than the total interaction if the motion is anisotropic. The fact that we do find an exponential decay of the magnetization and the measured $T_{1\rho}$ is much longer than the decay time of the FID supports that the perturbation method does give a good approximation.

Starting with the Hamiltonian just given, we first take the fluctuating part of the Hamiltonian

$$\Delta\mathcal{H} = \mathcal{H} - \langle\mathcal{H}\rangle = \omega_{CSA}\sum_m (-1)^m [D^{(2)}_{0-m}(\Omega) - \langle D^{(2)}_{0-m}\rangle]A^{lab}_{2m} \quad (10)$$

and then transform it into the doubly-rotating frame (we use $\langle \ldots \rangle$ to represent the average over the slow motion under consideration):

$$\begin{aligned}\Delta\mathcal{H}'' = \omega_{CSA}\Bigg\{&\frac{-1}{\sqrt{2}}[D^{(2)}_{01}(\Omega) - \langle D^{(2)}_{01}(\Omega)\rangle]\\ &\cdot\left[e^{i(\omega_0-\omega_1)t}d^{(1)}_{-11}\left(\frac{\pi}{2}\right)I_1 + e^{i\omega_0 t}d^{(1)}_{-10}\left(\frac{\pi}{2}\right)I_z + e^{i(\omega_0+\omega_1)t}d^{(1)}_{-1-1}\left(\frac{\pi}{2}\right)I_{-1}\right]\\ &+\frac{2}{\sqrt{6}}[D^{(2)}_{00}(\Omega) - \langle D^{(2)}_{00}(\Omega)\rangle]\\ &\cdot\left[e^{-i\omega_1 t}d^{(1)}_{01}\left(\frac{\pi}{2}\right)I_1 + d^{(1)}_{00}\left(\frac{\pi}{2}\right)I_z + e^{i\omega_1 t}d^{(1)}_{0-1}\left(\frac{\pi}{2}\right)I_{-1}\right]\\ &+\frac{-1}{\sqrt{2}}[D^{(2)}_{0-1}(\Omega) - \langle D^{(2)}_{0-1}(\Omega)\rangle]\\ &\cdot\left[e^{-i(\omega_0+\omega_1)t}d^{(1)}_{11}\left(\frac{\pi}{2}\right)I_1 + e^{-i\omega_0 t}d^{(1)}_{10}\left(\frac{\pi}{2}\right)I_z + e^{-i(\omega_0-\omega_1)t}d^{(1)}_{1-1}\left(\frac{\pi}{2}\right)I_{-1}\right]\Bigg\}. \quad (11)\end{aligned}$$

To simplify the Hamiltonian in the doubly rotating frame, we note that all terms which contain $e^{\pm i\omega_0 t}$ will only contribute to relaxation terms which are sensitive to fast motions only (with $\tau_c \approx 1/\omega_0$). The fast-motion relaxation rate can be estimated to be of the order of $1/T_1$ at 282 MHz, which is much smaller than $1/T_{1\rho}$ and is expected to have little locking-field or orientation dependence. So we drop those terms from now on and obtain

$$\Delta\mathcal{H}'' = \omega_{CSA}\frac{2}{\sqrt{6}}[D^{(2)}_{00}(\Omega) - \langle D^{(2)}_{00}(\Omega)\rangle]\cdot\left[\frac{e^{-i\omega_1 t}}{\sqrt{2}}I_1 + I_z + \frac{e^{i\omega_1 t}}{\sqrt{2}}I_{-1}\right]. \quad (12)$$

The rotating-frame relaxation rate, as induced by the slow motion, can be written as

$$\frac{1}{T_{1\rho}} = \int_0^\infty \langle[\Delta\mathcal{H}''(t-\tau), [\Delta\mathcal{H}''(t), I_z]]\rangle d\tau, \quad (13)$$

by substituting the Hamiltonian $\Delta\mathcal{H}''$ into Eq. 13 and using the commutation relations of spin operators, we obtain

$$\frac{1}{T_{1\rho}} = \frac{2}{3}\omega^2_{CSA}\int_0^\infty \{\langle D^{(2)}_{00}[\Omega(0)]D^{(2)*}_{00}[\Omega(\tau)]\rangle - |\langle D^{(2)}_{00}(\Omega)\rangle|^2\}\cos\omega_1\tau\, d\tau. \quad (14)$$

For every slow motion, there can be one or many components each with its own correlation time τ_c and all of them may induce relaxation at frequency ω_1. Assuming that the components with different correlation times can be treated independently, we have

$$T^{-1}_{1\rho} = \sum_i T^{-1}_{1\rho}(\tau_{ci}). \quad (15)$$

The rotation of Euler angle Ω can be expanded into two successive rotations. We will use $\Omega_1 = (\alpha_1, \beta_1, \gamma_1)$ to represent the Euler angle from the bilayer normal to the laboratory frame, which is time independent and determined only by the sample orientation during the experiment; then use $\Omega_2 = (\alpha_2, \beta_2, \gamma_2)$ to represent the Euler angle from the molecular axes to the bilayer normal which is randomly modulated by the slow motions under present consideration. Assuming that the correlation for each single motional component decays exponentially, we have

$$\begin{aligned}\langle D^{(2)}_{00}[\Omega(0)]D^{(2)*}_{00}[\Omega(\tau)]\rangle_i &= \sum_{n=-2}^{2}|D^{(2)}_{0n}(\Omega_1)|^2\cdot\langle D^{(2)}_{n0}[\Omega_2(0)]D^{(2)*}_{n0}[\Omega_2(\tau)]\rangle_i\\ &= \sum_{n=-2}^{2}|D^{(2)}_{0n}(\Omega_1)|^2\Big[(\langle|D^{(2)}_{n0}(\Omega_2)|^2\rangle_i - |\langle D^{(2)}_{n0}(\Omega_2)\rangle_i|^2)e^{-\tau/\tau_{ci}} + |\langle D^{(2)}_{n0}(\Omega_2)\rangle_i|^2\Big], \quad (16)\end{aligned}$$

where

$$\langle|D^{(2)}_{n0}(\Omega_2)|^2\rangle_i = \langle|d^{(2)}_{n0}(\beta_2)|^2\rangle_i = \begin{cases}\frac{1}{5} + \frac{2}{7}\langle P_2\rangle_i + \frac{18}{35}\langle P_4\rangle_i, & n = 0\\ \frac{1}{5} + \frac{1}{7}\langle P_2\rangle_i - \frac{12}{35}\langle P_4\rangle_i, & n = \pm 1\\ \frac{1}{5} - \frac{2}{7}\langle P_2\rangle_i + \frac{3}{35}\langle P_4\rangle_i, & n = \pm 2\end{cases} \quad (17a)$$

and

$$|\langle D^{(2)}_{n0}(\Omega_2)\rangle_i|^2 = \delta_{n0}|\langle d^{(2)}_{00}(\beta_2)\rangle_i|^2 = \delta_{n0}\langle P_2\rangle_i^2. \quad (17b)$$

The averages are defined as

$$\langle P_l\rangle_i = \int_0^{\pi} P_l(\cos\beta_2)\rho_i(\beta_2)\sin\beta_2 d\beta_2. \quad (18)$$

In the above equations, ρ_i and τ_{ci} represent the probability density and the correlation time of the i^{th} component of the slow motion, respectively. Substituting Eq. 17a and 17b into Eq. 16, we finally obtain

$$\frac{1}{T_{1\rho}} = \frac{2}{3}\omega^2_{CSA}\sum_i \int_0^{\infty}\left[\frac{1}{5}(1 - \langle P_4\rangle_i) + \frac{2}{7}P_2(\cos\beta_1)(\langle P_2\rangle_i - \langle P_4\rangle_i) + P_2^2(\cos\beta_1)(\langle P_4\rangle_i - \langle P_2\rangle_i^2)\right]e^{-\tau/\tau_{ci}}\cos\omega_1\tau\, d\tau. \quad (19)$$

2. Specific Model of Slow Motions

Unlike in simple crystals, there are many possible motions for a flexible lipid molecule in a liquid-crystalline-state bilayer. Because only simplified models can be solved analytically for the correlation function, we approximate the real motions by a superposition of several simple motions with different distributions of correlation times. In Fig. 1, we show a somewhat arbitrary decomposition of the overall motions into a number of "modes" which may still be incomplete. Assuming that the different "modes" are statistically uncorrelated, we can then separately discuss the relaxation caused by each. Motions which modulate only the intermolecular interactions (Fig. 1, *E–G*) will be excluded because both theory and dilution experiments have indicated that the relaxation we have observed is due to intramolecular processes. Also, the internal *trans-gauche* isomerization and the axial rotation of the entire molecule (Fig. 1, *A* and *B*) are expected to have a

Motion name	Picture	Character and Time scale (t_s)
(A) Trans-gauche isomerization		non-collective reorientation $t_s < 10^{-10}$ sec.
(B) Axial rotation		non-collective reorientation $t_s \approx 10^{-9}$ sec.
(C) Director fluctuation	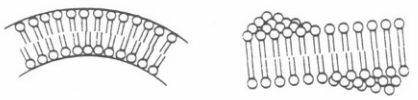	collective reorientation $t_s \approx 10^{-3}$ to 10^{-6} sec.
(D) Diffusion induced reorientation (near defects)	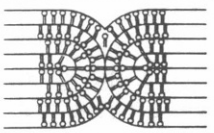	non-collective reorientation $t_s \approx$?
(E) Lateral diffusion	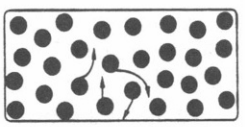	non-collective translation $t_s \approx 10^{-7}$ to 10^{-8} sec.
(F) Density fluctuation	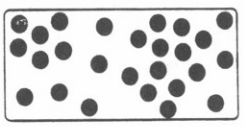	collective translation $t_s \approx$?
(G) Vertical motion (surface roughing)		? translation $t_s \approx$?

FIGURE 1 Schematic representations of various kinds of molecular motions that can exist in a bilayer structure.

correlation time much shorter than the $T_{1\rho}$ time scale. The remaining candidates for slow motions are:

(*a*) *Noncollective anisotropic reorientation due to diffusion on curved surface or near packing defects* (Fig. 1 *D*). This is a localized anisotropic reorientation of a single molecule which does not correlate with the motions of its far-away neighbors. Diffusion on a curved surface has been used by Bloom and Sternin (1987) to interpret their T_2 experiment. Here, we will include the diffusion around a packing defect also. Assuming that the reorientation has a relatively well-defined correlation time τ_c, this leads to

$$\frac{1}{T_{1\rho}} = \frac{2}{3}\omega_{CSA}^2\left[\frac{1}{5}(1 - \langle P_4\rangle) + \frac{2}{7}P_2(\cos\beta_1)(\langle P_2\rangle - \langle P_4\rangle) + P_2^2(\cos\beta_1)(\langle P_4\rangle - \langle P_2\rangle^2)\right]\frac{\tau_c}{1 + \omega_1^2\tau_c^2}. \quad (20)$$

An approximation often used is to assume that $\langle P_2\rangle = \langle P_4\rangle = S$ (Ukleja et al., 1976), which seems to be adequate for the diffusion-induced reorientation. Then Eq. 20 is simplified to

$$\frac{1}{T_{1\rho}} = \frac{2}{3}\omega_{CSA}^2(1 - S)\left[\frac{1}{5} + SP_2^2(\cos\beta_1)\right]\frac{\tau_c}{1 + \omega_1^2\tau_c^2}. \quad (21)$$

One should keep in mind that this order parameter, S, has no correlation with the fast motion order parameter S_{kl}^{FM}.

(*b*) *Director fluctuation, small collective disturbances with continuous spectrum of correlation times* (Fig. 1 *C*). These are wavelike disturbances which spread through the entire bilayer. The main characteristic of the director fluctuation is that each molecule only oscillates around its equilibrium position with a small amplitude. Director fluctuations have been studied extensively in nematic liquid crystals (Doane et al., 1974; Ukleja et al., 1976) and have been employed by several investigators to interpret the lipid-bilayer relaxation dispersion data (Pace and Chan, 1982; Brown, 1982; Brown et al., 1983 and 1986). To treat the continuous spectrum of correlation times, Σ_i will be replaced $1/(2\pi)^3\int_0^{q_c} 4\pi q\,dq$, where q is a wave vector. Since the fluctuation is small, one can expand the Legendre polynomial $P_l(\cos\beta_2)$ in a power series and keep only the leading non-zero term. That gives

$$\begin{cases}\langle P_2\rangle_q = 1 - \frac{3}{2}\langle|\beta_2(q)|^2\rangle \\ \langle P_4\rangle_q = 1 - 5\langle|\beta_2(q)|^2\rangle.\end{cases} \quad (22)$$

The relaxation rate is then given by

$$\frac{1}{T_{1\rho}} = \frac{2}{3}\omega_{CSA}^2\left(\frac{3}{2}\sin\beta_1\cos\beta_1\right)\cdot\int_0^{q_c=\infty}\left\{\int_0^{\infty} 3\langle|\beta_2(q)|^2\rangle e^{-\tau/\tau_q}\cos\omega_1\tau\,d\tau\right\}4\pi q\,dq = \frac{2}{3}\omega_{CSA}^2\left[\frac{3}{2}\sin\beta_1\cos\beta_1\right]\frac{3kT}{\pi K^{3/2}}\sqrt{\frac{\eta}{2}}\,\omega_1^{-1/2}, \quad (23)$$

where K is the elastic constant and η is the viscosity, k and T are the Boltzmann constant and absolute temperature, respectively.

3. Local Field Effects

The local field is a measure of the energy stored in the interacting spin system other than its Zeeman Hamiltonian (Wolf, 1979). The definitions of dipolar and CSA local fields are:

$$H_{LD}^2 = \frac{Tr\{(\mathcal{H}_D)^2\}}{\gamma^2\hbar^2\,Tr(I_z^2)},\ H_{LCSA}^2 = \frac{Tr\{(\mathcal{H}_{CSA})^2\}}{\gamma^2\hbar^2\,Tr(I_z^2)}. \quad (24)$$

In liquids, since the motion-averaged dipolar or CSA Hamiltonian vanishes, the local field is zero. Finite local fields are left for lipid bilayers because the complete motional average does not occur. For oriented bilayers, since we have shifted the transmitter frequency for every orientation, the CSA local field is automatically compensated. The CSA local field does complicate the interpretation of data from multilamellar liposomes, which we will discuss later as an off-resonance effect. In general, there are two effects caused by the local field.

The first effect is a change of the precession frequency for a particular spin, because the spin precesses not only in the Zeeman field, but also in the local field produced by its neighbors or other interactions. This effect can be taken into account by replacing the term ω_1 in our relaxation rate formula with $(\omega_1^2 + \omega_L^2)^{1/2}$, where ω_L is either the nonsecular part of or the total local field (in frequency units), depending upon the relative magnitude of the motional correlation time versus the thermal mixing time of the spin system (Wolf, 1979).

The second effect of the local field comes specifically from the local field produced by protons, which are not under spin-locking in our experiment. This can cause a cross-polarization of protons through the fluorine-proton spin–spin interaction (flip-flop), especially at the low locking field and for the orientations where local field is large (e.g., 0°). Hence, the relaxation rate that we have measured under those conditions will be larger than its true value, by which we mean the purely motion-induced relaxation. Right now, we do not have a method to calculate this effect accurately. However, we hope that the error brought by this effect is not very large because even for a solid phospholipid sample, the rotating-frame relaxation is still dominated by the motion-induced relaxation (Schaefer et al., 1984). Further studies aimed at ascertaining and eliminating this problem are currently in progress.

RESULTS

Fig. 2 *A* shows the 282.4 MHz ^{19}F NMR spectra of the oriented bilayers for different values of the orientation angle (β_1), which is defined as the angle between the bilayer director and the static magnetic field H_0. The

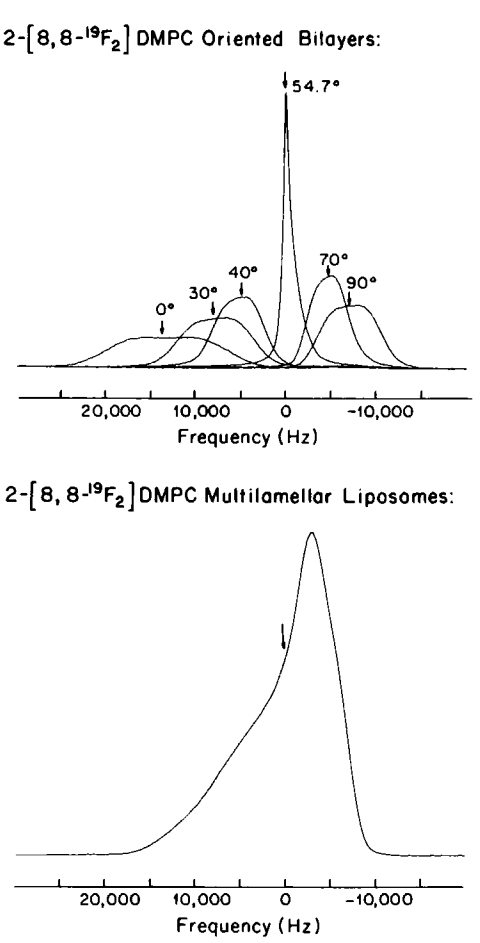

FIGURE 2 282.4 MHz ^{19}F NMR spectra of 2-[8,8-$^{19}F_2$]DMPC samples used in the relaxation studies. (*A*) Oriented bilayers; (*B*) multilamellar liposomes. Arrows indicate the transmitter frequency of the spin-locking pulse.

linewidth for the oriented bilayers comes from the F-F and F-H dipolar interactions which is scaled as $|P_2(\cos\beta_1)|$, and the center of the spectra is determined by the anisotropic chemical shift (Engelsberg et al., 1982). Fig. 2 *B* is the powder-pattern spectrum obtained for the multilamellar liposomes. The arrows on the spectra indicate the transmitter frequencies used for the locking pulse in relaxation measurements.

1. Rotating-Frame Relaxation of Oriented Bilayers

The locking-field dependence of the rotating-frame relaxation rate $T_{1\rho}^{-1}$ is displayed in Fig. 3, *A–C*. For all three isomers studied, at 0 and 90° orientations, fast decrease in the relaxation rate with an increase of the locking field has been observed in the low locking-field region. At the magic angle (54.7°) orientation, a much smaller but definite locking-field dependence has also been found. The differences between the relaxation rates at 0, 90, and 54.7° orientations decrease rapidly as the locking field is increased. Similar behavior of the relaxation rates has been reported by Cornell and Pope (1980) for the proton $T_{1\rho}^{-1}$ of unlabeled DMPC oriented bilayers, with the more pronounced field dependence region of their 0° data occurring at locking fields higher than we have observed here.

Fig. 4, *A–C*, show the orientation dependence of the $T_{1\rho}^{-1}$ for all three ^{19}F-labeled lipids at the 2-Gauss locking field. A large orientation dependence has been observed around the 0° orientation, while the relaxation rates are almost orientation independent between 50 and 90°. Our results show a similar shape but a larger change of relaxation time versus the sample orientation compared with the previous proton rotating-frame relaxation measurements (Pope et al., 1982). We have also noted that at different locking-field intensities, the orientation dependence changes shape, as illustrated in Fig. 5. This is a clue indicating that more than one motion may be present.

The magnitude of the relaxation rates depends on the labeling position, although both the locking-field and the orientation dependence are similar among the three isomers. The profile of $T_{1\rho}^{-1}$ along the acyl chain position is consistent with the spin-lattice relaxation rate T_1^{-1} profile (Brown and Seelig, 1979; Brown et al., 1983). In Table I, several representative relaxation rates are listed for each lipid. For comparison, one fast-motion order parameter along the F-F vector (S_{FF}^{FM}) measured from the dipolar splitting is also given for the same lipid sample.

At all locking fields and orientations, the relaxation rate decreases as the temperature is increased. For the 2-[8, 8-$^{19}F_2$] DMPC, the results are reported in Table II. The percentage change of the relaxation rate with temperature appears to be more or less independent of the locking field and orientation. The behavior of the other two isomers is essentially the same (results not shown). Care has been taken to change the sample temperature slowly, and the results are reproducible on both heating and cooling scans. (In one case, we have cooled the sample to 4°C, well below the phase transition temperature; after warming up, the same relaxation rate has been obtained.)

To verify the dominant relaxation mechanism, a dilution experiment (Fisher and James, 1978) was performed with 50 and 20% 2-[8, 8-$^{19}F_2$] DMPC diluted with perdeuterated DMPC-d_{54}. The same lipid alignment and NMR spectra were obtained from these samples as from the pure lipid samples, which ensure that the sample is homogeneous and single phased. The relaxation rates for the 0 and 90° orientations as a function of locking field, and for the 2-Gauss locking field as a function of orientation, measured on the diluted samples, are shown in Fig. 6, *A* and *B*. Compared with the pure sample, the change in the relaxation rates is no more than 10–15%. Because the intermolecular interactions will be scaled down upon dilution, while the intramolecular interactions will be unaffected, our results show that the intermolecular interactions do not make any significant contribution to the locking-field and orientation dependences of the relaxation rates.

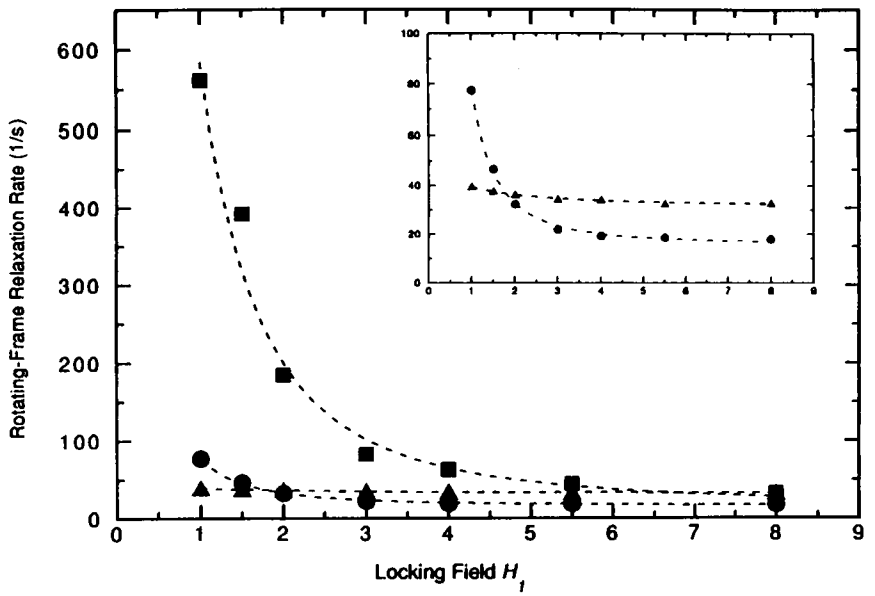

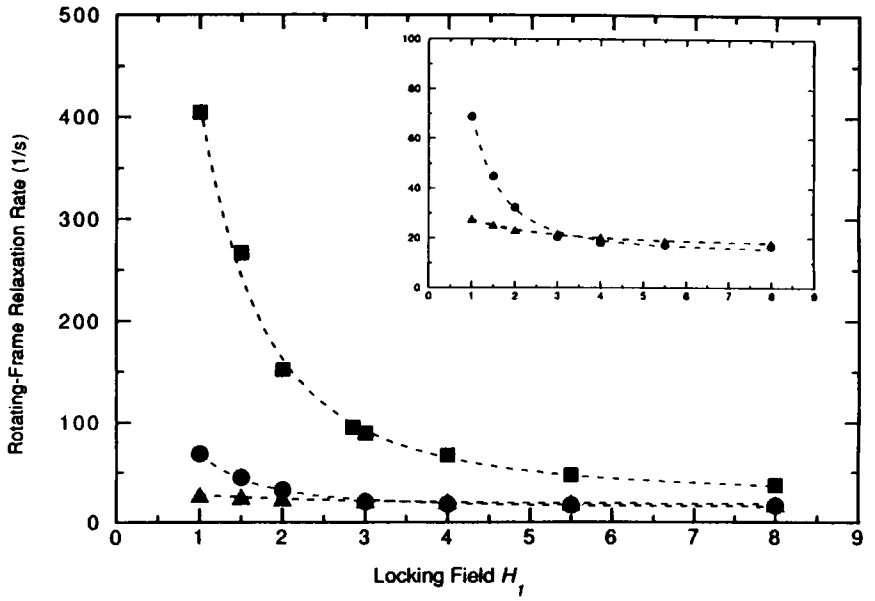

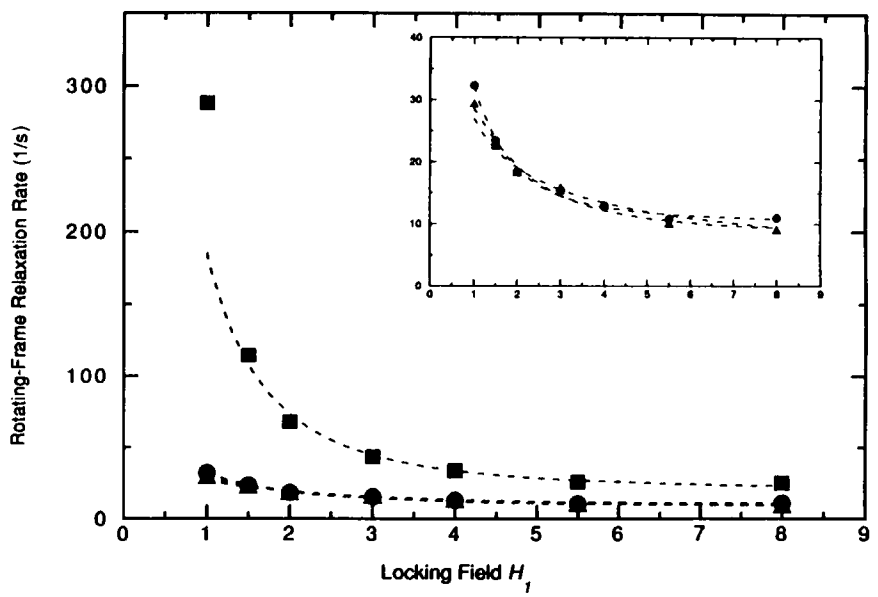

FIGURE 3 Locking-field dependence of the rotating-frame relaxation rate at 32°C for each ^{19}F-labeled phospholipid as oriented bilayers. (*A*) 2-[4,4-$^{19}F_2$]DMPC; (*B*) 2-[8,8-$^{19}F_2$]DMPC; (*C*) 2-[12,12-$^{19}F_2$]DPMC. (■) 0° orientation; (▲) 54.7° orientation; (●) 90° orientation. The lines are theoretical fits (see Discussion).

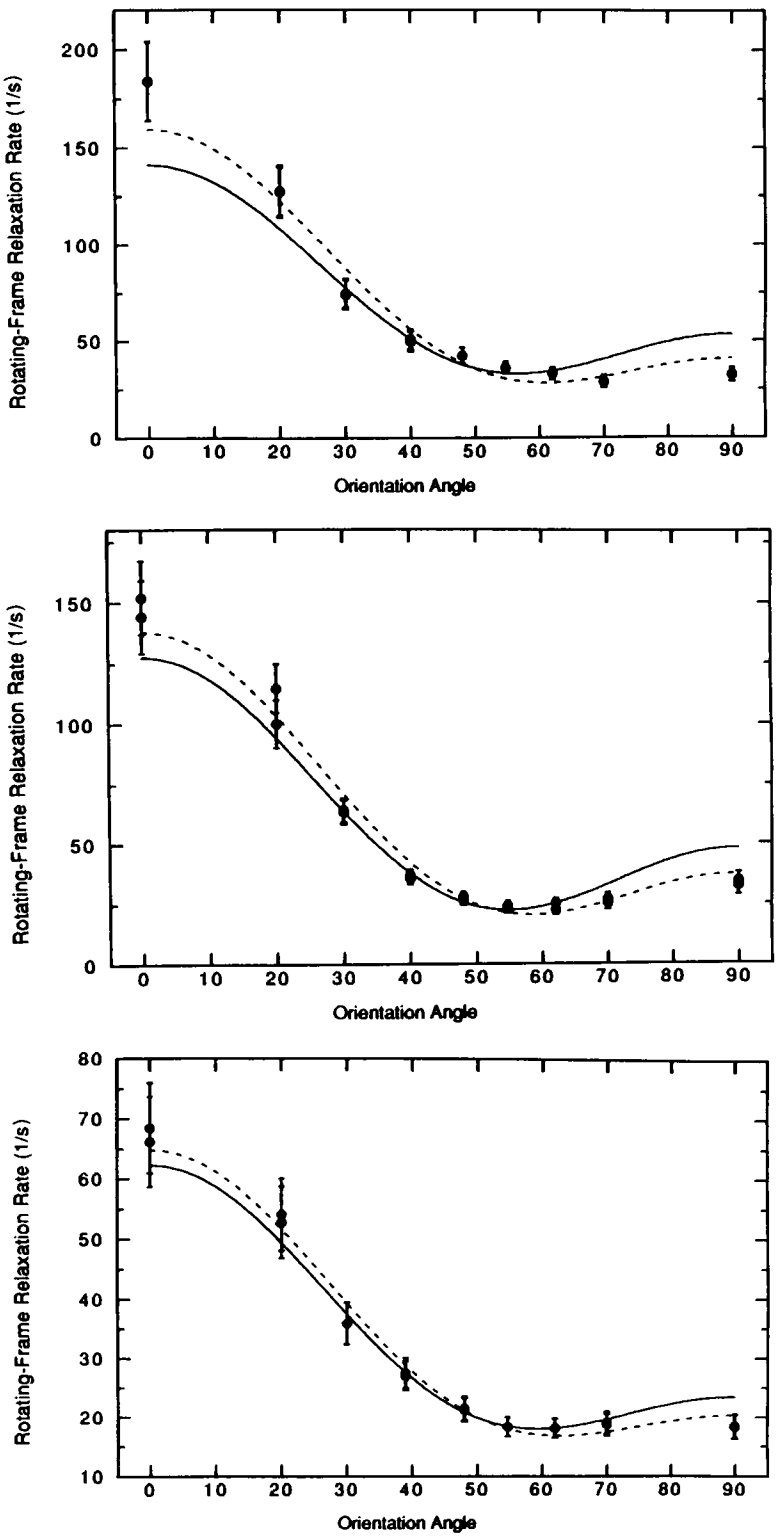

FIGURE 4 Orientation dependence of the rotating-frame relaxation rate at 32°C and 2-Gauss locking field for oriented ^{19}F-labeled lipid bilayers. (*A*) 2-[4,4-$^{19}F_2$]DMPC; (*B*) 2-[8,8-$^{19}F_2$]DMPC; (*C*) 2-[12,12-$^{19}F_2$]DMPC. The lines represent the best fits using a working theoretical model (see Discussion).

2. Rotating-Frame Relaxation of Multilamellar Liposomes

The relaxation rates have been measured also on the multilamellar liposomes as a function of the locking field. Although the transmitter frequency has been set to a value corresponding to the magic-angle component, because of the lateral diffusion of the lipid molecules one can measure only the orientation-averaged relaxation rates. In contrast to the oriented samples, there is no sharp locking-field dependence throughout the entire range (1–10 Gauss). The relaxation rates for all three isomers can be fitted well as a linear function of the inverse of the square root of the locking field ($1/T_{1\rho} = A + BH_1^{-1/2}$). This is shown in Fig.

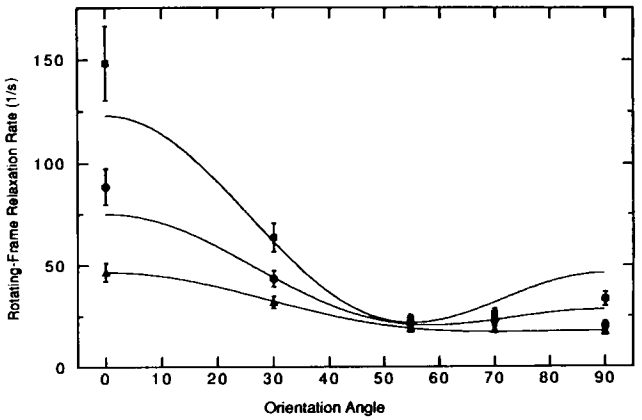

FIGURE 5 The change of the orientation dependence of the rotating-frame relaxation rate versus the locking-field strength for 2-[8,8-$^{19}F_2$]DMPC oriented bilayers. (■) H_1 = 2 Gauss; (●) H_1 = 3 Gauss; (▲) H_1 = 5.5 Gauss. The lines represent the best fits using a working theoretical model (see Discussion).

7, *A–C*. The field dependence that we have found coincides with the theory given by Pace and Chan (1982) for slow motions in multilamellar dispersion, and also with the T_1^{-1} dispersion data on small sonicated vesicles determined at higher frequencies by Brown et al. (1983), although the motions in small vesicles are not necessarily the same as in multilamellar liposomes. The data can be fitted neither by a simple Lorentzian function nor by the H_1^{-2} type of locking-field dependence.

The temperature dependence of the relaxation rate is always small for multilamellar liposomes except for the case of 2-[4, 4-$^{19}F_2$] DMPC, and for that the direction of the temperature dependence is opposite to that of the oriented bilayers (see Fig. 7 *A*). The weak locking-field and temperature dependence seems to indicate that the motions in the liposome are substantially different from those in the oriented samples, as will be discussed below. Nevertheless, the general molecular packing is expected to

TABLE I
^{19}F-LABEL POSITION DEPENDENCE
OF THE ROTATING-FRAME RELAXATION RATE
OF ORIENTED LIPID BILAYERS AT 32°C, FOR 2-GAUSS
AND 8-GAUSS LOCKING FIELDS

Locking field	Orientation	$^{19}F\ T_{1\rho}^{-1}$ (s^{-1})		
		2-[4,4-$^{19}F_2$]	2-[8,8-$^{19}F_2$]	2-[12,12-$^{19}F_2$]
	degrees	s^{-1}	s^{-1}	s^{-1}
2 Gauss	0	184	152	67.3
	54.7	36.0	23.6	18.4
	90	32.3	32.3	18.3
8 Gauss	0	32.5	36.8	25.2
	54.7	32.8	17.7	11.0
	90	17.9	16.6	9.1
Order parameter (S_{FF}^{FM})		0.244	0.238	0.156

A comparison with the order parameter (S_{FF}^{FM}) profile is also included.

TABLE II
TEMPERATURE DEPENDENCE
OF THE ROTATING-FRAME RELAXATION RATE
OF ORIENTED 2-[8,8-$^{19}F_2$]DMPC LIPID BILAYERS
AT VARIOUS ORIENTATIONS AND LOCKING FIELDS

Orientation	Locking field	$^{19}F\ T_{1\rho}^{-1}$		
		27°C	32°C	39°C
degrees	*Gauss*	s^{-1}	s^{-1}	s^{-1}
0	1	625	500	455
	2	183	141	106
	4	85.5	58.8	41.2
	8	51.5	33.8	23.9
90	1	80.0	62.1	45.5
	2	38.0	29.2	18.9
	4	23.7	16.9	12.9
	8	21.9	16.4	11.4
54.7	2	26.0	19.1	14.1
	8	23.2	17.7	12.4

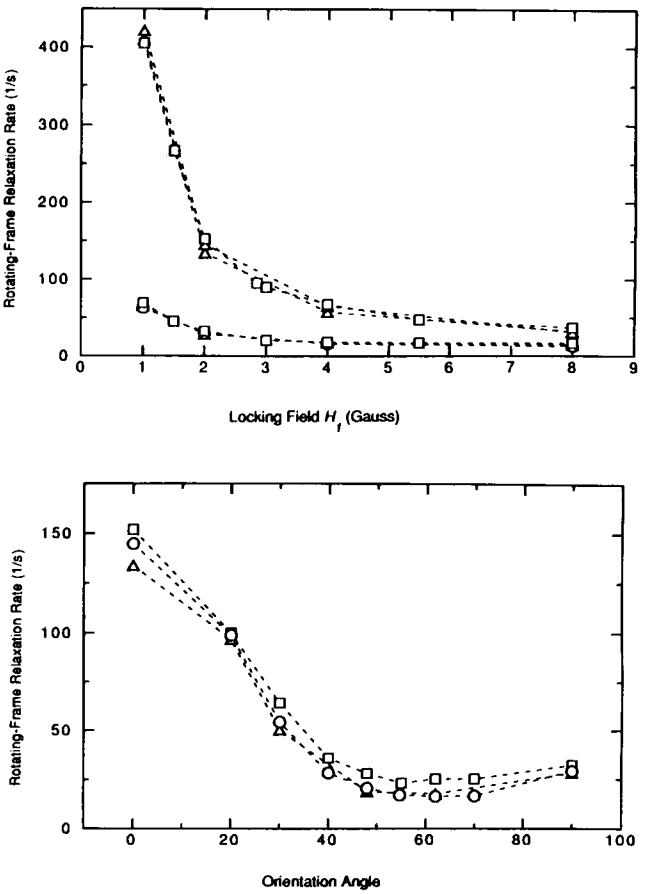

FIGURE 6 The rotating-frame relaxation rate for the diluted oriented bilayers: (*A*) Locking-field dependence; (*B*) the orientation dependences. (□) 100% 2-[8,8-$^{19}F_2$]DMPC; (△) 50% 2-[8,8-$^{19}F_2$]DMPC + 50% DMPC-d_{54}; (○) 20% 2-[8,8-$^{19}F_2$]DMPC + 80% DMPC-d_{54}.

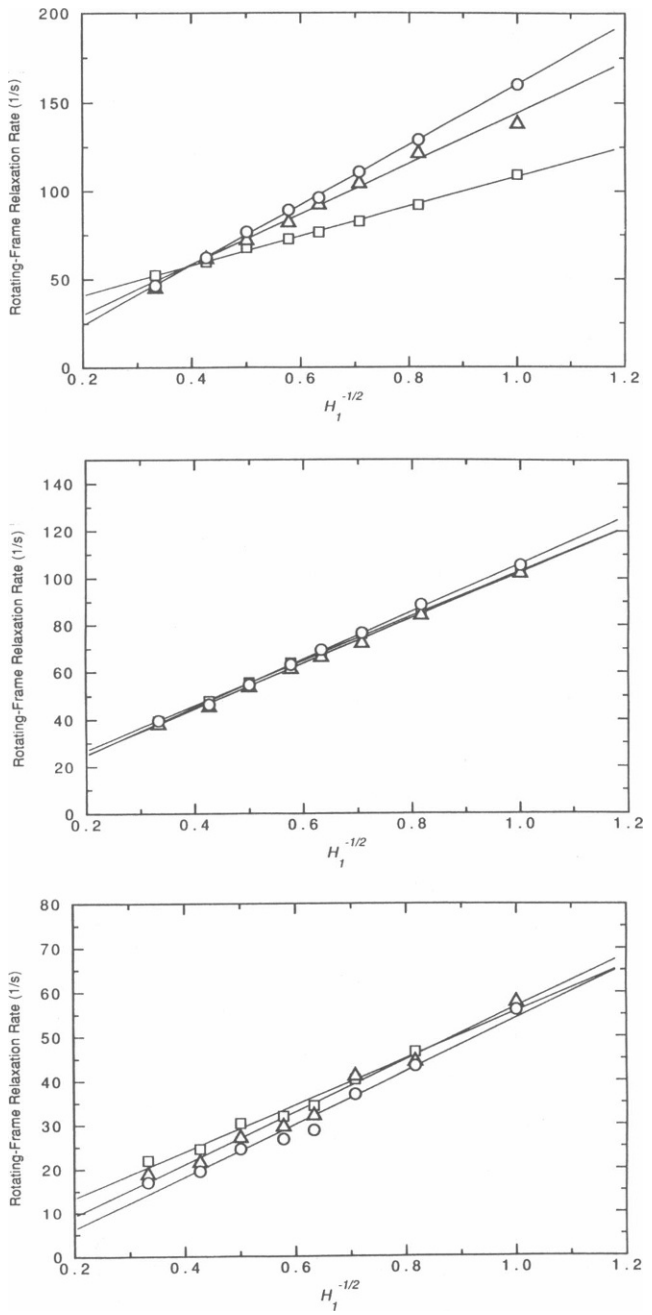

FIGURE 7 Locking-field and temperature dependences of the rotating-frame relaxation rate for ^{19}F-labeled phospholipid multilamellar liposomes as a function of the inverse square root of the locking field. (*A*) For 2-[4,4-$^{19}F_2$]DMPC; (□) 32°C; (△) 39°C; (○) 46°C; (*B*) for 2-[8,8-$^{19}F_2$]DMPC; (□) 32°C; (△) 39°C; (○) 46°C; (*C*) for 2-[12,12-$^{19}F_2$]DMPC; (□) 25°C; (△) 32°C; (○) 39°C.

be similar in these two forms, because the label position dependence of $T_{1\rho}^{-1}$ is about the same.

DISCUSSION

1. Existence of Slow Motion(s)

It is well known that the difference between $T_{1\rho}$ and T_1 indicates the amount of motions which have their frequency spectra lying between ω_1 and ω_0. For both the oriented bilayer and the multilamellar liposome samples, the spin-lattice relaxation time of ^{19}F is ~300–400 ms. This is much longer than the observed $T_{1\rho}$, which ranges from 5 to 50 ms in most cases. In agreement with previous studies, our results have confirmed that there are extensive "slow" motions in the phospholipid model membranes. By "slow," we mean that the correlation time of the motion is much longer than the time scale defined by the Larmor frequency encountered usually in NMR studies (about 10^{-9} s). The details of the slow motions, however, are quite different between the two types of model membranes that were used in our investigations. In the following, we will only discuss the properties of the slow motions having their frequency spectrum covered by our locking-field range, namely, from 10^{-4} to 10^{-6} s.

2. Orientation Dependence

In Fig. 8, we have plotted the theoretical orientation dependence for both anisotropic reorientation (via diffusion) and director fluctuation. For the case of oriented bilayers, one can immediately see from the orientation dependence of the relaxation rate that the motions can be essentially described by the anisotropic reorientation model and not by the director fluctuation model. To account for the details of the orientation dependence and, especially, the changes in the orientation dependence at different locking fields, it appears that the presence of other types of motion is required. Because identical curves have been obtained either by fitting the data using our general formula, Eq. 19, or by using a superposition of one anisotropic reorientation term plus another director fluctuation term, we would like to propose the following working model.

$$\frac{1}{T_{1\rho}}(\beta_1)^{Total} = R_1 A_{AR}(\beta_1) + R_2 A_{DF}(\beta_1)\,, \qquad (25)$$

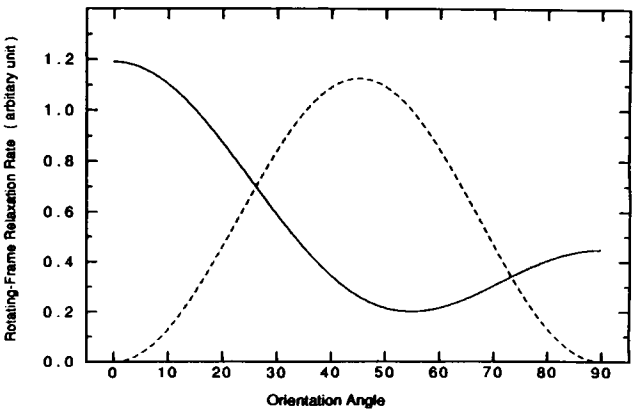

FIGURE 8 Theoretical orientation dependence of $T_{1\rho}^{-1}$ calculated from the pure large-scale anisotropic reorientation (via lateral diffusion on curved surface or near packing defects) (*solid line*) and the pure director fluctuation (*dashed line*).

where $A_{AR}(\beta_l)$ and $A_{DF}(\beta_l)$ are given by (c.f., Eqs. 21 and 23):

$$\begin{cases} A_{AR}(\beta_l) = 1/5 + SP_2^2(\cos\beta_l), \\ A_{DF}(\beta_l) = 3/2 \sin^2\beta_l \cos^2\beta_l \end{cases} \quad (26)$$

R_1 and R_2 are orientation-independent relaxation rates induced by each type of motion (however, they do depend on the locking field). No correlation between the two motions has been assumed (for a rigorous treatment, see Freed, 1977).

The best fits for the orientation dependence using this working model are included in Fig. 4, *A–C* and Fig. 5 (*solid lines*), where we can see that the fitting is much better under higher locking field. We currently think that the mismatch between the theoretical model and the experiment is due to fluorine-proton cross-polarization through the local field. By adding an extra term $R_{FH}(\beta_l)$ which is proportional to $P_2^2(\cos\beta_l)$, as the averaged fluorine-proton interaction would be to Eq. 25, we can improve our fitting (in Fig. 4, *A–C, broken lines*). It is worth noting that to fit the experimental data, one has to use a large order parameter ($S \approx 1$) in the anisotropic reorientation term. This means that the reorientations are highly anisotropic, so that the time-averaged molecular orientation is close to a perfect alignment. This is expected for motions in such an anisotropic medium. (Again, one should not confuse the order parameter for this particular slow reorientation with the fast motion order parameter, S^{FM}). Our working model also predicts that the director fluctuation tends to give a larger contribution at higher H_1 field because it has a weaker H_1 dependence, whereas at lower locking fields, the anisotropic reorientation term would have a larger weight. All these features are consistent with the observed changes of the orientation dependence versus the locking field (c.f., Fig. 5).

3. Field Dependence for Oriented Bilayers

For the locking-field dependence at the 0 and 90° orientations, because there is no contribution from the director fluctuation term, our working model predicts that the locking field dependence of relaxation rate should be fitted by an anisotropic reorientation alone, which has been assumed to have a well-defined correlation time. The strong field dependence at low locking fields indicates that the reorientation has a long correlation time. Unfortunately, the region (1–1.5 Gauss) that shows significant locking-field dependence falls into the area where the proton local field may cause significant loss of magnetization, which has also been found experimentally at 0° orientation. In Table III, we listed the apparent correlation time fitted by using the Lorentzian function given by Eq. 21 and the local filed itself estimated from the magnetization loss at low locking fields. Curves are included in Fig. 3, *A–C*. One should not take the exact value of these correlation times too seriously, although the order of magnitude is probably correct.

TABLE III
APPARENT CORRELATION TIMES OBTAINED FROM FITTING THE LOCKING-FIELD DEPENDENCE DATA OF THE RELAXATION RATE AT 0°, 90°, AND 54.7° ORIENTATIONS FOR EACH OF THE LIPIDS IN ORIENTED BILAYER FORM

Label position	Orientation	τ_c	Local field
	degrees	*s*	*Gauss*
2-[4,4-$^{19}F_2$]	0	6×10^{-5}	≈1.0*
	90	1×10^{-4}	≈0.55
	54.7	2.5×10^{-5}	0
2-[8,8-$^{19}F_2$]	0	5×10^{-5}	≈1.0
	90	6×10^{-5}	≈0.55
	54.7	2×10^{-5}	0
2-[12-12-$^{19}F_2$]	0	5×10^{-5}‡	≈0.6
	90	4×10^{-5}	≈0.3
	54.7	2.5×10^{-5}	0

Fitting with the Lorentzian function as given by Eq. 21. The values of the dipolar local field are estimated from the loss of magnetization at low locking field.
*Estimated error, ~10%.‡ The 1-Gauss point was excluded in the fitting.

At the 54.7° orientation, lesser contribution from anisotropic reorientation and significant contribution from director fluctuation is expected. We find that the small-field dependence can be fitted by either Eq. 21 or Eq. 23 or a combination of the two; a unique determination of the functional form is impossible. These results are also included in Fig. 3, *A–C*, and Table III. (In principle, the correlation times obtained from different sample orientations should be the same, the differences are probably due to local field effect again.)

The correlation times that we have obtained are longer than those reported by Cornell and Pope (1980). There are several factors that may account for the difference. First, Cornell and Pope (1980) used egg-yolk lecithin (EYL), which itself is a mixture of lipids; this heterogeneity may introduce extra motions. Second, the reduced temperature for our measurement is much lower than that for their case, because of the extremely low phase transition point for EYL. Third, the water content of our sample is probably lower than theirs, and it is known that the water content can affect the motional properties of the acyl chain (Tanaka and Freed, 1984; and our unpublished results).

4. Effect of Temperature Change on Oriented Bilayers

We are aware that the decrease of the relaxation rate when temperature increases observed for the oriented bilayer samples, even after correcting for the decrease of ω_{CSA}, indicates that the motion is in the short correlation time regime ($\omega_1\tau_c < 1$). However, the value of our fitted correlation time implies that the same motion is in the long correlation time regime ($\omega_1\tau_c > 1$). If the correlation time

is longer than $1/\omega_1$ at some locking field values and follows the usual thermal activation, the relaxation rate should increase with increasing temperature. One possibility is that there may be a broad $T_{1\rho}$ minimum due to distributed correlation times, another interpretation is that the temperature dependence is mainly due to a decrease in the number of relaxation centers, rather than to a change in the correlation time. The second interpretation supports the idea that the anisotropic reorientation found in the oriented bilayers is related to the presence of packing defects.

5. A Possible Molecular Origin for the Localized Reorientation

Except for the values of the correlation time, our results from the specifically labeled oriented lipid bilayers are similar to the earlier results reported by Cornell and co-workers (Cornell and Pope, 1980; Pope et al, 1982), both for the field and the orientation dependence. However, they interpreted the relaxation mechanism as a modulation of intermolecular interactions, which we have found not to be applicable to our systems, and which is further disproved by the dilution experiment. We find that the anisotropic reorientation which we have discussed must be intramolecular with a time scale about or greater than 10^{-5} s, so that the internal rotations around the carbon–carbon bond (*trans-gauche* isomerization) are unlikely to be the answer. A motion of the entire molecule is generally slower because of the larger mass and greater geometrical constraints. This motion also must involve a large scale reorientation in contrast with the small director fluctuation. Large scale reorientation is most likely to be localized in space and not very collective. From all these considerations and from the temperature dependence of the relaxation rate and the fact that very different results are obtained from parallel studies of multilamellar liposomes (*vide infra*), we propose that the anisotropic reorientation in the oriented bilayers originates from the diffusion around packing defects in the bilayer. The dotlike defects which we have observed with the polarizing microscope are a possible source, and there are probably other, smaller defects which cannot be seen by optical microscopy (e.g., about the size of 10 bilayers). It is known that the number of certain kinds of defects actually decreases as the temperature rises (annealing), and therefore the relaxation rate could decrease. Finally, although the relaxation may originate from defects, the relaxation data are reproducible (within ~10%) for different samples prepared independently.

6. Comparison with Multilamellar Liposomes

In the case of multilamellar liposomes, we do see a qualitatively different locking-field and temperature dependence under the same experimental conditions as for the oriented bilayers. Both the weak $H_1^{-1/2}$ locking-field dependence and the small temperature effect are consistent with the model of collective director fluctuation (Pace and Chan, 1982; Brown 1982). Because in the liposome sample there is excess water and there are fewer constraints on the molecular packing, it is plausible that the motion which dominates the low-frequency nuclear relaxation is not the same as in the oriented bilayers, especially if the number of packing defects is expected to be much less. In terms of our working model, this means that the first term now is small, and the second term for liposomes is larger than for the oriented bilayers.

The theories given by Pace and Chan (1982) and by Brown (1982) are essentially the same. However, the detailed experimental studies by Brown and co-workers have been done only on the high-frequency end with small vesicles. Only very recently, the low-field proton spin-lattice relaxation on multilamellar liposomes has been measured (Rommel et al., 1988), and their results support the director fluctuation model plus an additional motion. Independently, they suggested the diffusion over curved surfaces or defects as a supplemented motional mechanism.

The locking-field dependence of $T_{1\rho}$ on most nuclei other than proton has to be interpreted with caution for unoriented samples, because only those lipid molecules which are at the magic-angle orientation relative to the static field are exactly on-resonance, and the molecules which are off-resonance will have a relaxation rate dependent on the off-resonance angle. As an approximate check, we have integrated numerically the theoretical relaxation rates over the solid angle, while assuming that the molecules are equally distributed on a perfect sphere. In the calculation, we have used $\omega_{eff} = (\omega_1^2 + \Delta\omega^2)^{1/2}$ instead of ω_1 and the corresponding expression for the orientation dependence of $\Delta\omega = 2\pi\nu\ (3\cos^2\beta - 1)/2$, where $\nu = 13.3$ KHz is the reduced CSA strength as measured from the frequency difference between the 0° orientation and magic angle orientation. The results show that none of the models gives an exactly linear relaxation rate against $\omega_1^{-1/2}$, and that different models are not clearly distinguishable in the locking-field range available for performing these experiments.

7. Label Position Dependence of the Relaxation Rate

It is known that the shape of the label position profile of the spin-lattice relaxation rate is similar to the shape of the fast-motion order parameter profile, and the relaxation rate is approximately proportional to the square of S^{FM} (Brown and Seelig, 1979; Brown et al., 1983). In the case of $T_{1\rho}$, which reflects slower motions, the label-position profile has not been established. Ideally, the relaxation rate should be proportional to the square of the effective spin-lattice interaction (Williams et al., 1985), ω_{CSA}, which in turn is proportional to the fast-motion order parameter,

S^{FM}. In our work, the fast-motion order parameter, S_{FF}^{FM}, given in Table I, is the experimental counterpart of S^{FM}. However, our observations show that $T_{1\rho}^{-1}$ seems to be proportional to S_{FF}^{FM} itself rather than to its square. This disagreement might exist because the time scales of the motions reflected by $T_{1\rho}$ and S_{FF}^{FM} are different, and because the theoretical treatments are not detailed enough.

CONCLUDING REMARKS

This work is an attempt to study the relaxation mechanism of the CF_2 group functioning as a probe in phospholipid bilayers and to correlate our results with the results of earlier experiments by other groups. Our dilution experiments clearly rule out the fluctuation of intermolecular interactions as a significant relaxation pathway for the ^{19}F nucleus. This allows us to eliminate several possible motions as the source of relaxation. For the oriented bilayers, we have found that there is a slow motion which can be described by a large-scale localized anisotropic reorientation of the ^{19}F-bearing segment with a long correlation time. We have suggested the diffusion around certain kind of packing defects as a possible mechanism for this reorientation. Evidence of more than a single motion that is responsible for the low-frequency relaxation has also been found. The difference in defect population may account for the differences between the behavior of the oriented bilayers and the multilamellar liposomes. The slow motions in the multilamellar liposomes are most likely to be collective, as represented by the director fluctuation, although more evidence is necessary to prove it.

Our results do show that the relaxation rate is sensitive to the label position. Since there are more fast motions, and the environment becomes more isotropic near the bilayer mid-plane, the relaxation rate decreases towards the tail of the chain. Nevertheless, as far as the slow motions are concerned, many features of our results do not change with the label position, except for their numerical value. This indicates that the entire molecule is involved in slow motion rather than certain segments only. Our results agree qualitatively with many of the results obtained previously from averaged proton relaxation. This is also an indication that the CF_2 group does not perturb the bilayer structure significantly.

In conclusion, ^{19}F-labeled lipids offer a new possibility to investigate motional properties in various membrane systems. It is expected that by adding other membrane-interacting components, such as cholesterol or peptides, to the bilayer, we will be able to observe specific motional changes in the acyl-chain region.

We would like to thank Dr. A. A. Bothner-By, Dr. S. I. Chan, Dr. J. Schaefer, and Dr. M. Bloom for helpful discussions, and Dr. S. R. Dowd for synthesizing the lipids. The polarizing microscopy experiment was carried out with the assistance of Dr. F. Lanni.

This work is supported by research grants from the National Institutes of Health (GM-26874 and HL-24525) and the National Science Foundation (DMB 85-121451). During 1985–87, I.J.L. was supported by a senior fellowship awarded by the National Institutes of Health (GM-80251) while spending his sabbatical leave in the Department of Biological Sciences at Carnegie Mellon University.

Received for publication 5 October 1987 and in final form 7 March 1988.

REFERENCES

Abragam, A. 1961. The Principles of Nuclear Magnetism. Clarendon Press, Oxford. 264–322.

Asher, S. A., and P. S. Pershan. 1979. Alignment and defect structures in oriented phosphatidylcholine multilayers. *Biophys. J.* 27:393–421.

Blicharski, J. S. 1972. Nuclear magnetic relaxation by anisotropy of the chemical shift. *Z. Naturforsch.* 27:1456–1458.

Bloom, M., and E. Sternin. 1987. Transverse nuclear spin relaxation in phospholipid bilayer membranes. *Biochemistry.* 26:2101–2105.

Brown, M. F., and J. Seelig. 1979. Structural dynamics in phospholipid bilayers from deuterium spin-lattice relaxation time measurement. *J. Chem. Phys.* 70:5045–5053.

Brown, M. F. 1982. Theory of spin-lattice relaxation in lipid bilayers and biological membranes. ^2H and ^{14}N quadrupolar relaxation. *J. Chem. Phys.* 77:1576–1599.

Brown, M. F., A. A. Ribeiro, and G. D. Williams. 1983. New view of lipid bilayer dynamics from ^2H and ^{13}C NMR relaxation time measurement. *Proc. Natl. Acad. Sci. USA.* 80:4325–4329.

Brown, M. F., J. F. Ellena, C. Trindle, and G. D. Williams. 1986. Frequency dependence of spin-lattice relaxation times of lipid bilayers. *J. Chem. Phys.* 84:465–470.

Campbell, R. F., E. Meirovitch, and J. H. Freed. 1979. Slow-motional NMR line shapes for very anisotropic rotational diffusion. Phosphorus-31 NMR of phospholipids. *J. Phys. Chem.* 83:525–533.

Cornell, B. A., and J. M. Pope. 1980. Low frequency and diffusive motion in aligned phospholipid multilayers studied by pulsed NMR. *Chem. Phys. Lipids.* 27:151–164.

Cornell, B. A., J. B. Davenport, and F. Separovic. 1982. Low-frequency motion in membranes: the effect of cholesterol and proteins. *Biochim. Biophys. Acta.* 689:337–345.

Davis, J. H. 1983. The description of membrane lipid comformation, order and dynamics by ^2H-NMR. *Biochim. Biophys. Acta.* 737:117–171.

Doane, J. W., C. E. Tarr, and M. A. Nickerson. 1974. Nuclear spin-lattice relaxation in liquid crystals by fluctuations in the nematic director. *Phys. Rev. Lett.* 33:620–624.

Dowd, S. R., V. Simplaceanu, and C. Ho. 1984. Fluorine-19 nuclear magnetic resonance investigation of fluorine-19-labeled phospholipids. 2. A line-shape analysis. *Biochemistry.* 23:6142–6146.

Engelsberg, M., S. R. Dowd, V. Simplaceanu, B. Cook, and C. Ho. 1982. Nuclear magnetic resonance line-shape analysis of fluorine-19-labeled phospholipids. *Biochemistry* 21:6985–6989.

Feigenson, G. W., and S. I. Chan. 1974. Nuclear magnetic relaxation behavior of lecithin multilayers. *J. Am. Chem. Soc.* 96:1312–1319.

Fisher, R. W., and T. L. James. 1978. Lateral diffusion of the phospholipid molecule in dipalmitoylphosphatidylcholine bilayers. An investigation using nuclear spin-lattice relaxation in the rotating frame. *Biochemistry.* 17:1177–1183.

Freed, J. H. 1977. Stochastic-molecular theory of spin-lattice relaxation for liquid crystal. *J. Chem. Phys.* 66:4183–4199.

Griffin, R. G. 1981. Solid state nuclear magnetic resonance of lipid bilayers. *Methods Enzymol.* 72:108–173.

Ho C., S. R. Dowd, and J. F. M. Post. 1985. ^{19}F NMR investigations of membranes. *Curr. Top. Bioenerg.* 14:53–95.

Huang, T. H., R. P. Skarjune, R. J. Wittebort, R. G. Griffin, and E. Oldfield. 1980. Restricted rotational isomerization in polymethylene chains. *J. Am. Chem. Soc.* 102:7377–7379.

Kimmich, R., G. Schnur, and A. Scheuermann. 1983. Spin-lattice relaxation and lineshape parameters in nuclear magnetic resonance of lamellar lipid systems: fluctuation spectroscopy of disordering mechanisms. *Chem. Phys. Lipids.* 32:271–322.

Pace, R. J., and S. I. Chan. 1982. Molecular motions in lipid bilayers. II. Magnetic resonance of multilamellar and vesicle systems. *J. Chem. Phys.* 76:4228–4240.

Pope, J. M., L. Walker, B. A. Cornell, and F. Separovic. 1982. A study of the angular dependence of NMR relaxation times in macroscopically oriented lyotropic liquid crystal lamellar phases. *Mol. Cryst. Liq. Cryst.* 89:137–150.

Post, J. F. M., B. W. Cook, S. R. Dowd, I. J. Lowe, and C. Ho. 1984. Fluorine-19 nuclear magnetic resonance investigation of fluorine-19-labeled phospholipid. 1. A multiple-pulse study. *Biochemistry.* 23:6138–6141.

Rommel, E., F. Noack, P. Meier, and G. Kothe. 1988. Proton spin relaxation dispersion studies of phospholipid membranes. *J. Phys. Chem.* In press.

Schaefer, J., M. D. Sefcik, E. O. Stejskal, and R. A. McKay. 1984. Carbon-13 $T_{1\rho}$ experiments on solid polymers having tightly spin-coupled protons. *Macromolecules.* 17:1118–1124.

Seelig, J., and A. Seelig. 1980. Lipid conformation in model membranes and biological membranes. *Q. Rev. Biophys.* 13:19–61.

Smith, R. L., and E. Oldfield. 1984. Dynamic structure of membranes by deuterium NMR. *Science (Wash. DC).* 225:280–288.

Tanaka, H., and J. H. Freed. 1984. Electron spin resonance studies on ordering and rotational diffusion in oriented phosphatidylcholine multilayers: evidence for a new chain-ordering transition. *J. Phys. Chem.* 88:6633–6644.

Ukleja, P., J. Pirs, and J. W. Doane. 1976. Theory for spin-lattice relaxation in nematic liquid crystals. *Phys. Rev. A.* 14:414–423.

Williams, G. D., J. M. Beach, S. W. Dodd, and M. F. Brown. 1985. Dependence of deuterium spin-lattice relaxation rates of multilamellar phospholipid dispersions on orientational order. *J. Am. Chem. Soc.* 107:6868–6873.

Wolf, D. 1979. Spin-Temperature and Nuclear-Spin Relaxation in Matter. Clarendon Press, Oxford.

Wu, W. G., S. R. Dowd, V. Simplaceanu, Z.-y. Peng, and C. Ho. 1985. ^{19}F NMR investigation of molecular motion and packing in sonicated phospholipid vesicles. *Biochemistry.* 24:7153–7161.